RSC Advances

ROYAL SOCIETY OF CHEMISTRY

www.rsc.org/advances

RSC Advances

RSCPublishing

ARTICLE

Enantioselectively bioreductive preparation of chiral halohydrins employing two newly identified stererocomplementary reductases

Cite this: DOI: 10.1039/xoxxoooooox

Guo-Chao Xu,[a,b] Hui-Lei Yu,*[a] Yue-Peng Shang[a] and Jian-He Xu*[a]

Received ooth January 2012,
Accepted ooth January 2012

DOI: 10.1039/xoxxoooooox

www.rsc.org/

Two robust stererocomplementary carbonyl reductases (*Dh*CR and *Cg*CR) were identified through rescreening the carbonyl reductases toolbox. Firstly, five reductases were returned through the activity and enantioselectivity assay to α-chloro-1-acetophenone and ethyl 4-chloro-3-oxo-butanate (COBE). Secondly, three reductases were proved to be stable at elevated substrate loading. Thirdly, enzymatic characterization revealed that *Dh*CR and *Cg*CR were more thermostable. As much as 330 g COBE in 1 L biphasic reaction mixture were effectively reduced into (*S*)- and (*R*)-CHBE employing *Dh*CR and *Cg*CR (coexpressed with glucose dehydrogenase), with 92.5% and 93.0% yields, >99% *ee* and total turnover numbers of 53800 and 108000 respectively. Six other α-halohydrins were asymmetrically reduced into optically pure forms at substrate loading of 100 $g \cdot L^{-1}$. All indicate the potential of these two stererocomplemenatry reductases in the synthesis of valuable α-halohydrins in pharmaceuticals.

Introduction

Asymmetric reduction of prochiral ketones is one of the most important, fundamental and practical reactions for production of chiral secondary alcohols, which can be transformed into various functionalities of industrial relevance such as pharmaceuticals, agrochemicals and natural products.[1] Optically active α-halogenated alcohols constitute important building blocks in the synthesis of pharmaceutical and liquid crystal products.[2] Most importantly, the two opposite enantiomers may have similar, different or even opposite effects. For example, ethyl (*S*)-3-hydroxy-4-chlorobutyrate ((*S*)-CHBE) is a key chiral precursor for HMG-CoA reductase inhibitors to lower cholesterol, while (*R*)-CHBE is an important intermediate for L-carnitine which acts as an antioxidant.[3–4] Both enantiomers of 2-chloro-1-(2',4'-dichlorophenyl)ethanol could be applied in the synthesis of antifungal agents, such as miconazole, econazole, and sertaconazole, however, with different antifungal profiles and activities.[5] Hence the enantioselective preparations of both enantiomers of α-halohydrins are of equal importance.

Modern manufacturing industries appeal for efficient, green, energy-saving and environmental benign procedures.[6] The discovery and application of biocatalysts applied in the chemical synthesis, especially for value-added products, do pump new vitality due to their specially and complicatedly spatial, electronical and polar structures.[7] All the inherently properties of enzymes endue them high diversity and enantioselectivity, easy operation, environmental benign and high atom economy.[8] Dramatically improvement has been achieved employing enzymes, accompanied with arise of the third wave of biocatalysis.[9]

Since the demanding diversity in the biomanufacture, there is a constant need of new biocatalysts with altered performance, such as high catalytic efficiency, wide substrate scope, high regio- and enantioselectivity, thermo- and pH-stability and tolerance against high substrate/product/organic solvent.[10] For a certain reaction, classical enrichment cultivation was regarded as the effective strategy to identify original microorganisms harboring active enzymes evolved by nature. Based on this, various new and efficient tools at disposal have been established and opened up new avenues to shorten the period for discovery of enzymes with desired properties, including metagenome, shotgun/insertion mutation, genome database mining, isolation and purification approaches from the original microorganisms.[11] Recently, great achievement has been made with genome database mining, which was referring to the screening of enzymes similar in sequences with target-reaction-oriented screen and selection. Recombinant DNA technology has enabled the rapid increase in accessible genome data (currently at a rate of *ca.* 200 per month), providing more and more sequences with unknown functions and promoting the quick identification of naturally-evolved enzyme libraries by genome mining.[12] Various strategies have been published in the prediction and rational selection of genes from genome database.[13] However less was focus on the strategies to identify robust and enantioselective enzymes.

Table 1 Enzymes identified through genome data mining

	Enzyme	EC[a]	Candidate[b]	Characteristics [Substrate, Loading /g·L^{-1}, *ee* /%, S. T. Y. /g·L^{-1}·d^{-1}][c]	Ref
1	*Sc*CR	1	10	COBE, 600, >99, 304	[15]
2	*Cg*KR1	1	8	CBFM, 300, >98.7, 261	[16]
3	*Cg*KR2	1	13	OPBE, 206, >99, 700	[17]
4	*Kt*CR	1	30	CAPE, 154, >99, 283	[18]
5	*Ar*QR	1	17	QNCO, 242, >99, 916	[19]
6	*Es*LeuDH	1	15	TMP, 78.1, >99, 275	[20]
7	*Ba*NTR1	1	24	CNB, 14.8, >99 sel., 291	[21]
8	rPPE01	3	17	APA, 64.8, 99, 97.2	[22]
9	*La*N	3	13	CMN, 50.2, 96.5, 143	[23]
10	*Ba*E	3	22	MDPEA, 40, 97, 38.6	[24]

[a] EC classification, 1 as oxidoreductase, 3 as hydrolase; [b] Numbers of candidates; [c] S. T. Y.: Space-time yield. Substrates: COBE (ethyl 4-chloro-3-oxo-butanate), CBFM (methyl *o*-chlorobenzoylfomate), OPBE (ethyl 3-oxo-phenylbutanate), CAPE (*α*-chloro-1-acetophenone) QNCO (3-quinuclidinone), CNB (4-cyanonitrobenzene), APA (*α*-acetoxyphenyl acetate), MDPEA (1-(3',4'-methylenedioxyphenyl) ethyl ester), CMN (*o*-chloromandelonitrile).

To work as an alternative to chemical synthesis in industrial scale, one biocatalyst should possess certain properties, such as tolerance against no less than 100 g·L^{-1} substrate, >99% enantioselectivity, high operational stability, none byproduct and <0.1 g·L^{-1} cofactor addition.[14] Our group have being committed to the discovery and engineering of robust enzymes with promising potentials in organic synthesis of chiral building blocks with pharmaceutical relevance as shown in **Table 1**. An NADH-dependent carbonyl reductase *Sc*CR has been identified from *Streptomyces coelicolor* with substrate-coupled cofactor regeneration, and the specific production rate was 36.8 $g_{product}/g_{dry\text{-}cell\text{-}weight}$ in the asymmetric preparation of key chiral precursor for atorvastatin (Lipitor®).[15] For the synthesis of chiral *o*-chloromandelic acids, key building blocks for clopidogrel (Plavix®), two biocatalysts, an NADPH-dependent ketoreductase *Cg*KR1 and an novel nitrilase *La*N have been discovered from *Candida glabrata* and *Labrenzia aggregata*.[16, 23] The space-time yield of them could reach >100 g·L^{-1}·d^{-1}, through the asymmetric reduction of methyl *o*-chlorobenzoylformate (CBFM) and enantioselective resolution of *o*-chloromandelonitrile (CMN) respectively. However, based on our previously results in genome mining as illustrated in **Table 1**, one biocatalyst with desired characteristic was obtained out from 8–30 candidates (rejection rate was >87.5%). Nonetheless, most of the genes were neglected and little was known on the detailed properties, ascribing to the sole screen and selection criteria, generally activity and enantioselectivity towards the target substrate. In our previous work, only one substrate-tolerant carbonyl reductase *Kt*CR was screened out of 30 potential reductases for the preparation chiral halohydrins from *α*-chloro-1-acetophenone (CAPE, **4**).[18] We supposed that the others might display similar or even higher catalytic performance. To rescreen this library for robust reductases, a new three rounds of screening strategy was proposed, covering activity and enantioselectivity to substrates with altered substituents as primary screening, operational stability against substrate/product and thermostability. The application potential in the enantioselectively preparation of halohydrins was also investigated.

Results and discussion

Rescreening result with COBE as substrate

A carbonyl reductases' toolbox was developed for robust haloketone reductases. In our primary screening using **4** as target substrate, only three carbonyl reductases (*Kt*CR, *Pg*CR and *Cl*CR) were returned with relatively higher activity (>0.5 U·mg^{-1}) and enantioselectivity (>99%).[18] Among them, the highest activity was determined with *Cl*CR (1.5 U·mg^{-1}). Further comparison at increased substrate loading revealed the instability of *Pg*CR and *Cl*CR, and only *Kt*CR was selected out (**Table 2**). Most of the candidates were eliminated due to their low activity. However, when the screening substrate was altered to ethyl 4-chloro-3-oxobutanate (COBE, **22**), an *α*-halogenated *β*-ketoester, resulted in a different profile. Twelve reductases were proved with specific activity of more than 0.5 U·mg^{-1}, which was higher than that tested with **4**. The exciting results encouraged us to analyze the enantioselectivity in the asymmetric reduction of **22** and **4**. *Dh*CR and *Cg*CR, from *Debaryomyces hansenii* (Uniprot accession no. Q6BQ25) and *Candida glabrata* (Q6FR42), displayed stable performance, even at 200 mM of **4** (**Table 2**). Especially in the case of *Dh*CR, the time and catalyst requirement were much less than *Kt*CR, although the apparent specific activity of *Dh*CR was only 38% of *Kt*CR, indicating that low apparent activity has little connection with the biotransformation efficiency. *Cg*CR was the only reductase with Prelog preference in the asymmetric reduction of prochiral ketones among all the candidates. Reductases with relatively higher activity were more liable to be instable in the enantioselectivity. Hash conditions, *i.e.* high reagent concentration (substrate or product) and high temperature, might affect their structural conformation and lead to the decrease of activity and enantioselectivity. Considering the activity and *ee* to two screening substrates, *Dh*CR and *Cg*CR were regarded as interested reductases, besides *Kt*CR. Hence, for the primary screening for activity and operational stability in genome data mining, adoption of at least two types of substrates with similar structure was better to comprehensively understand the candidates' performance. However, other characteristics, such as the substrate profiles toward different kinds of substrates and enzyme performance (thermostability), were also needed to be considered.

Enzymatic characteristic of three carbonyl reductases

Three recombinant reductases with *N*-terminal His-tag were purified to electrophoretic homogeneity by nickel affinity chromatography. The specific activity to **22** of the purified *Dh*CR, *Kt*CR and *Cg*CR was 13, 11 and 8.0 U·mg^{-1} respectively. Protein separation of purified enzyme by SDS-

Figure 1 Screening results of the 30 carbonyl reductases

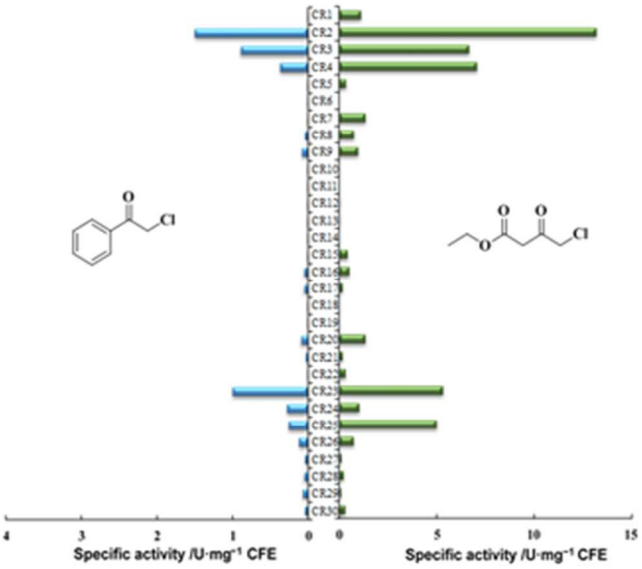

employing two haloketones (**4** and **22**) with different substituents. Blue columns: activities towards CAPE, green columns: activities towards COBE.

Table 2 Asymmetric reduction of *α*-chloroacetophenone with the five best carbonyl reductases.

Enzyme	Substrate [mM]	Catalyst [kU/L]	Time [h]	Conv. [%]	*ee* [%]/[*R*/*S*]
	10	1	12	>99	>99 /*S*
*Cl*CR	100	10	12	>99	95.6 /*S*
	200	40	24	80.8	80.0 /*S*
	10	1	12	>99	>99 /*S*
*Kt*CR	100	10	12	>99	>99 /*S*
	200	20	12	>99	>99 /*S*
	10	1	12	>99	>99 /*S*
*Pg*CR	100	10	12	>99	92.4 /*S*
	200	40	24	76.6	60.5 /*S*
	10	1	6	>99	>99 /*S*
*Dh*CR	100	10	6	>99	>99 /*S*
	200	10	6	>99	>99 /*S*
	10	1	12	>99	98.7 /*R*
*Cg*CR	100	10	12	>99	98.6 /*R*
	200	20	8	>99	98.7 /*R*

PAGE resulted in a single band corresponding to a molecular weight of 34, 35 and 40 kDa (**Fig. S1**), in agreement with their theoretical values. Gel exclusion chromatography with TSK G2000 SWx1 column shown a single peak of *Dh*CR, *Kt*CR and *Cg*CR with an elution volume corresponding to an apparent molecular mass of 67.2 69.6 and 39.8 kDa, respectively, which indicated that they were homodimeric and momomeric enzymes.

Effect of pH and temperature on the activity of three carbonyl reductases were investigated as shown in **Fig. S2**. All displayed the highest activity at around pH 6.5. The optimum temperature of *Dh*CR and *Cg*CR were 55 and 60, 45°C for *Kt*CR according to the temperature-profiles. Activity of *Cg*CR decreased rapidly over 60°C due to the thermal inactivation. For *Dh*CR and *Cg*CR, the relative activity at 30°C was 70.8% and 27.0% of the activity at optimum temperature. Thermal stabilities were investigated at different temperatures. The half-lives of *Kt*CR, *Dh*CR and *Cg*CR at 30, 40 and 50°C were 18, 462 and 169 h, 11.8, 111 and 80.6 h, 0.16, 2.1 and 1.3 h as shown in **Table 3**. *Dh*CR and *Cg*CR were stable at 30°C and 40°C, but liable at higher temperatures. The deactivation energy (E_a) of *Dh*CR and *Cg*CR were 218±6 kJ·mol^{-1} and 198±8 kJ·mol^{-1} respectively, while that of *Kt*CR was 190±8 kJ·mol^{-1}. All above indicated that *Dh*CR and *Cg*CR were much more stable at room and elevated temperatures.[26]

The kinetic constants of the purified reductases to CAPE (**4**) and COBE (**22**) were calculated from the Lineweaver-Burk double-reciprocal plot as shown in **Table 3**. The k_{cat} to **22** of *Dh*CR and *Cg*CR was 16.6 s^{-1} and 27.9 s^{-1} respectively. Relative low K_M value to NADPH (<50 μM) of *Dh*CR and *Cg*CR could guarantee the high efficiency even under no addition of external cofactors (**Table S3**). Although the k_{cat} values to **4** of *Dh*CR and *Cg*CR were lower than *Kt*CR, they were much more efficient in the asymmetric reduction of COBE and quite stable against high temperature. The substrate specificity and catalytic performance in the preparation of chiral halohydrins of them were further investigated.

Table 3 Comparison on the enzymatic characteristics of *Kt*CR, *Dh*CR and *Cg*CR.

Characteristic		*Kt*CR	*Dh*CR	*Cg*CR
Molecular weight /kD		69.8	67.2	39.8
Numbers of subunit		2	2	1
Optimal pH		6.5	6.5	6.5
Optimal temperature /°C		45	55	60
Thermostability	30°C	18.0	462	169
/h	40°C	11.8	111	80.6
	50°C	0.163	2.09	1.26
Ea /kJ·mol^{-1}		190±5	218±6	198±3
CAPE, 4	K_M /mM	2.3±0.2	2.1±0.1	2.2±0.1
	k_{cat} /s^{-1}	7.3±0.3	4.0±0.2	1.6±0.1
COBE, 22	K_M /mM	3.2±0.1	1.3±0.1	3.7±0.2
	k_{cat} /s^{-1}	13.2±0.2	16.6±0.3	27.9±0.4

Substrate profiles of stererocomplementary *Dh*CR and *Cg*CR

No activity with NADH, but full activity with NADPH was detected using purified *Dh*CR and *Cg*CR (data not shown), indicating both were NADPH dependent carbonyl reductases. Twenty five prochiral ketones (numbered from **1** to **25**) with various substituents, covering aromatic and aliphatic ketones and *β*-ketoesters, were selected to characterize the substrate spectra of *Dh*CR and *Cg*CR.

As shown in **Fig. 2**, different substrate profiles were observed with *Dh*CR and *Cg*CR. Among the tested substrates, no evident preference was discovered with *Dh*CR, while *Cg*CR preferred *β*-ketoesters to aromatic and aliphatic ketones. Along

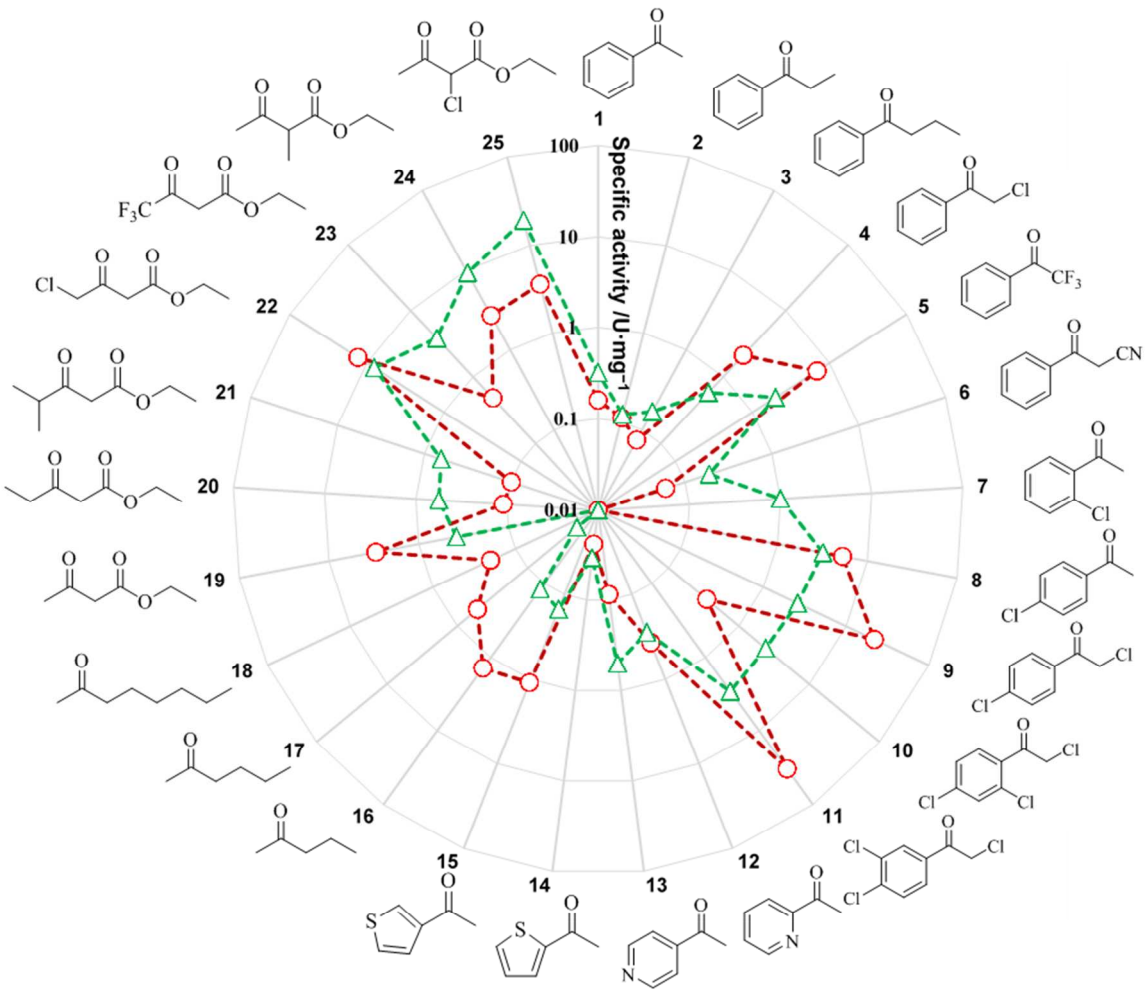

Figure 2 Substrate profiles of *Dh*CR (○) and *Cg*CR (Δ). Specific activities are shown in logarithmic form in the radar map. The activities equal or lower than 0.01 U·mg^{-1} purified protein are shown as 0.01 U·mg^{-1}. Detailed values are listed in **Table S4** in ESI.

with the increase of side-chain length of aromatic ketones, from acetophenone to 1-butyrophenone (**1**–**3**), the specific activity of *Dh*CR gradually decreased. *Cg*CR displayed higher catalytic activity to 1-butyrophenone than 1-propiophenone. Due to the electron-imbalance, *α*-substituted acetophenone derivatives (**4**–**6**, **9**–**12**) were easier to be reduced by reductases. Although the CN was a strong electron-withdrawing group, benzoylacetonitrile (**6**) was hard to be reduced due to the steric hindrance of CN group. 2'-chloroacetophenone (**7**) was usually poor substrate for carbonyl reductases. However *Cg*CR displayed relatively higher activity toward **7**. The specific activity ratio of 4'-chloroacetophenone (**8**) to **7** of *Cg*CR was 3.2, much lower than 88.3 of *Dh*CR, indicating that *Cg*CR could accept much larger aromatic ketones with ortho-substituents on phenyl ring. Compared with aryl ketones, heteroaryl ketones were more difficult to be reduced. Aliphatic ketones were better substrates for *Dh*CR than *Cg*CR, implying an application potential of them in the preparation of chiral aliphatic secondary alcohols. *Cg*CR showed higher activity to *β*-ketoesters than *Dh*CR, especially to ethyl 4,4,4-trifluro-3-oxo-butonate (**23**). Highest activity of *Dh*CR was found towards 2,3',4'-trichloroacetophenone (**11**, 33 U·mg^{-1}). With regard to *Cg*CR, ethyl 2-chloro-3-oxo-butonate (**25**, 19 U·mg^{-1}) was the best among all the tested substrates. Interestingly, opposite enantioselectivity-preference was detected with *Dh*CR than *Cg*CR, although low enantioselectivity was observed with *Cg*CR to several substrates (20–98%, **Table S4**). In the asymmetric reduction of prochiral ketones, *Dh*CR obeyed anti-Prelog rule while *Cg*CR complied with Prelog priority. The preparation of both enantiomers of chiral *α*-halohydrins, which were usual of equal importance, could be achieved with these two stereocomplementary reductases.

In the regions conserved between *Dh*CR and SDR proteins, *Cg*CR and AKR members, the typical SDR and AKR sequence motifs, such as cofactor binding, catalytic, substrate binding and structure stabilizing residues, were found as illustrated in **Table S1** and **Figure S4** & **S5**.[27] It was indicated that *Dh*CR and *Cg*CR belonged to SDR and AKR family respectively. Further consensus analysis with homologous proteins shown that they were members of SDR51C and AKR1B10 subfamily based on online database nomenclature search (http://www.sdr-enzymes.org/, http://www.med.upenn.edu/akr/).[28]

A characteristic glycine-rich Rossmann-fold scaffold was found in the *N*-terminal of *Dh*CR for the binding of $NADP^+$ dinucleotide.[29] The Rossmann-fold sequence in *Dh*CR was TGSSGGIGWA, sharing the both motif of the 'classical' or 'extended' subfamily. Because the length of 'extended family' was 30-residue longer than the 250 amino acid residues of 'classical' type SDR, and also *Dh*CR had the conserved adenine ring binding and active site motifs of 'extended' subfamily (**Table S2**). All above implied that *Dh*CR was a member of 'extended' group.

No Rossmann-fold scaffold motif was found in *Cg*CR. However, as shown in **Table S1**, typical motifs of AKR were all found in *Cg*CR, which indicated that *Cg*CR was a potential member of AKR superfamily.[30] Among all the consensus sequences, catalytic tetrad, Asp-Tyr-Lys-His (50-55-80-111), appeared in *N*-terminal of *Cg*CR. Thr26, Asp50, Asn167, Gln190, Ser263 and Arg268 played important role in cofactor binding. Other residues, such as Gly23, Gly25, Gly45, Asp106, Pro113, Gly165 and Pro187, might play structural roles in the forming the barrel core, since they were found within the β-strands, α-helices and short loops regions of the barrel.

Optimization on the asymmetric reduction of COBE into chiral CHBEs

*Dh*CR and *Cg*CR were coexpressed with glucose dehydrogenases separately to provide cofactor regeneration systems. The catalytic performances in the asymmetric reduction of COBE (**22**) into optically active CHBE with *Dh*CR and *Cg*CR were systematically studied as shown in **Table S6**. *Dh*CR could asymmetrically reduce substrate **22** into (*S*)-CHBE, an important synthon for statin side chain, while (*R*)-CHBE was produced with *Cg*CR aiming for L-carnitine. It was stated that **22** was not stable at aqueous phase, especially in alkaline condition, and may be toxic to biocatalysts.[31] Biphasic system was usually applied to minimize the losses of substrate and product. Since in toluene/aqueous system, the partition coefficient of **22** and CHBE were 21.3 and 2.8 respectively, and also *Dh*CR, *Cg*CR and *Bm*GDH retained high activity, toluene was selected as the organic phase.[25] The intracellular amount of $NADP^+$ was also quantified to calculate TTN of these two complementary reductases. And there was 1.86±0.13 μmol $NADP^+$ in one gram DCW of *E. coli* BL21 (**Table S5**), which was a little higher than the reported around 0.39−0.79 $\mu mol \cdot g^{-1}$ DCW.[32] Less than 0.1 $\mu mol \cdot g^{-1}$ of NADPH was detected. While 0.44±0.02 $\mu mol \cdot g^{-1}$ DCW NAD^+ was calculated in vivo of *E. coli* BL21. There was less difference between *E. coli* BL21 harbouring *Dh*CR and *Cg*CR coding genes.

High substrate loading was the request for practical application, usually at more than 100 $g \cdot L^{-1}$. Hence the optimization was carried out in order to increase the substrate concentration and total turnover number (TTN) of reductases in toluene/aqueous biphasic system. Within 6 h, 0.2 M of **22** were asymmetrically reduced with >99% conversion employing 10 $g \cdot L^{-1}$ *Dh*CR and 5 $g \cdot L^{-1}$ *Cg*CR. Along with the increase of substrate/catalyst ratio, as much as 330 $g \cdot L^{-1}$ (660 $g \cdot L^{-1}$ in toluene phase) of **22** could be fully reduced with no addition of external cofactor (**Table S6**). Up-scaled preparation of (*S*)- and (*R*)-CHBE was carried out at 1 L scale, 330 g of **22** were added in 0.5 L toluene phase and fully reduced within 24 h (**Figure 3**). After purification, the molar isolation yield of (*S*)- and (*R*)-CHBE was calculated to be 92.5% and 93.0% respectively, ee_p was >99%. The substrate to catalyst (S/C) ratios were 33 for *Cg*CR and 16.5 for *Dh*CR.

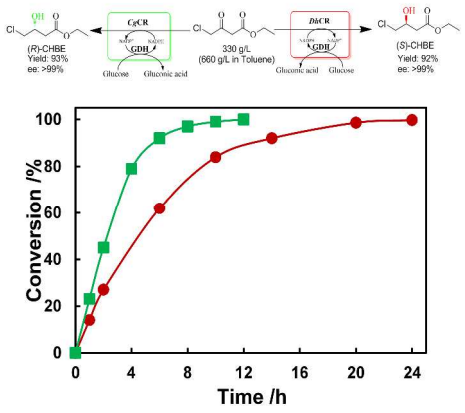

Figure 3 Asymmetric reduction of 330 g COBE to both enantiomers of chiral CHBE with *Dh*CR and *Cg*CR at 1 L reaction mixture (toluene/aqueous biphasic system).

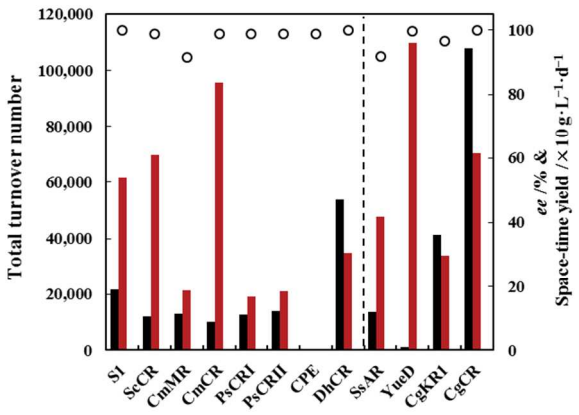

Figure 4 Comparison of the catalytic performance of selected ketoreductases in the asymmetric reduction of COBE into chiral CHBE. Black bar (■): total turnover number, red bar (■): space-time yield, hollow cycle (○): *ee*.

As shown in **Figure 4** and **Table S7**, lots of research had been focused on the preparation of (*S*)-CHBE, due to its wide application in the preparation of statin side-chain of pharmaceutical relevance. All the (*S*)-isomers produced reductases belonged to SDR family. Except for CmMR from *Candida magnolia*, most of them displayed excellent enantioselectivity. Highest records of substrate loading and TTN of cofactor were achieved with carbonyl reductase *Sc*CR and CmS1 from *Streptomyces coelicolor* and *C. magnolia*.[15, 31, 33] However the requirement of external cofactor was disadvantageous for the wide application in organic synthesis.

Table 4 Efficiently bioreductive preparation of various chiral halohydrins at high substrate loading.

Substrate	*Dh*CR					*Cg*CR					Chiral blocks in pharmaceutical relevant products
	Concn. [g·L^{-1}]	Catal.[a] [g·L^{-1}]	Time [h]	Yield [%]	*ee* [%]/[*R*/*S*]	Concn. [g·L^{-1}]	Catal.[b] [g·L^{-1}]	Time [h]	Yield [%]	*ee* [%]/[*R*/*S*]	
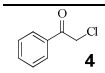 **4**	100	30	24	88	>99 /*S*	30.8	20	24	85	98 /*R*	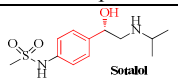 Sotalol
 **5**	174	30	24	90	>99 /*S*	–[d]	–	–	–	–	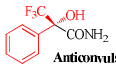 Anticonvulsant
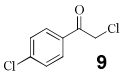 **9**	189	30	24	89	>99 /*S*	94.5	20	24	90	>99 /*R*	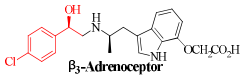 β$_3$-Adrenoceptor
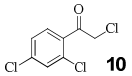 **10**	44.4	30	12	89	>99 /*S*	100	20	12	88	>99 /*R*	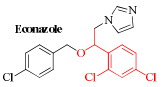 Econazole
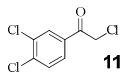 **11**	100	30	12	90	>99 /*S*	100	20	24	87	>99 /*R*	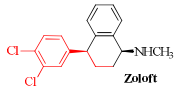 Zoloft
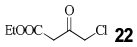 **22**	330 (660)[d]	20	24	92	>99 /*S*	330 (660)[d]	10	12	93	>99 /*R*	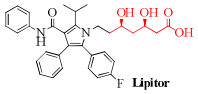 Lipitor
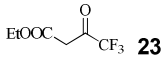 **23**	184	30	24	89	>99 /*S*	184	10	24	92	>99 /*R*	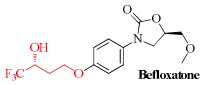 Befloxatone

[a] Catalyst, dry cells of recombinant *E. coli* BL21/pET28-*bmgdh-dhcr*; [b] Catalyst, dry cells of recombinant *E. coli* BL21/pET28-*bmgdh-cgcr*; [c] Reaction was not implemented due to the low ee value (54%); [d] 330 g·L^{-1} in the reaction mixture and 660 g·L^{-1} in organic phase.

Under no assistance of exogenous NADP$^+$, as much as 330 g·L^{-1} could be asymmetrically reduced within 24 h employing recombinant *Dh*CR, which provided a much more efficient and green reductase for the preparation of chiral (*S*)-CHBE. The TTN and space-time yield (STY) of *Dh*CR was 53800 and 305 g·L^{-1}·d^{-1} respectively, calculated based on intracellular NADP$^+$/NADPH. Comparing to (*S*)-isomers, relatively less reductases had been reported for the produce of (*R*)-CHBE. A carbonyl reductase from *Sporobolomyces salmonicolor*, *Ss*CR, could catalyze full reduction of 300 g·L^{-1} of **22**, however, only with 91.7% (*R*) *ee*.[34] Among all the (*R*)-isomers producing reductases, YueD from *Bacillus subtilis* was reported with the highest *ee* value at 214 g·L^{-1} substrate loading (fed-batch), however, in the assistance of 1 mM NADP$^+$,[35] which would burden its cost and hinder its application. With no aid of external cofactor, for the first time, 330 g·L^{-1} of **22** were asymmetrically reduced into optically pure (*R*)-CHBE. The S/C, TTN and STY of *Cg*CR were 33, 108000 and 614 g·L^{-1}·d^{-1} respectively.

Enzymatic preparation of both enantiomers of halohydrins

High substrate specificity was the important characteristic of biocatalysts. Different substituents at different positions may endue substrates with district properties, such as electricity, hydrophobicity, polarity and spatiality. Unlike classical chemical catalysts, tremendous difference on biocatalysts was usually found with diverse substrates. The catalytic activity and enantioselectivity may vary according to the changes of substrates. An ideal reductase should not only display high activity and enantioseletivity, but also have high substrate tolerance and, most importantly broad substrate scope. Although "one for all" was impossible for enzymes, as an efficient alternative tool in organic synthesis of chiral compounds, a serials of substrates owning similar functional groups should also be catalyzed. Several α-substituted prochiral ketones with high activity and enantioseletivity in the substrate spectra analysis of *Dh*CR and CgCR were chosen out to test the applicability.

All of the tested substrates could be reduced at 100 g·L^{-1} substrate loading into optically pure α-halohydrins as illustrated in **Table 4**.All the α-halohydrins were important chiral building blocks with pharmaceutical relevance, for example, (*S*)-α-chloro-1-acetophenol could be used for sotalol,[36a] (*S*)-2,2,2-trifluroacetophenol for liquid crystals and anticonvulsant pharmaceuticals,[36b, 36c] (*S*)-2,4'-dichloroacetophenol for adrenergic receptor agonists,[36d] (*S*)-2,3',4'-trichloroacetophenol for sertraline,[36e] (*R*)-2,2',4'-trichloroacetophenol for econazole,[5] ethyl (*R*)-4,4,4-trifluro-3-hydroxybutyrate for befloxatone,[36f] etc. The efficient preparation the optically pure α-halohydrins provides key evidences for the application potential of *Dh*CR and *Cg*CR.

Conclusions

In summary, through rescreening and characterization, two robust haloketone reductases (*Dh*CR and *Cg*CR) were identified from recently developed carbonyl reductases' toolbox. Generally, activity and enantioselctivity were the key cariteria in the chiral biocatalysis. In previously work, a

carbonyl reductase *Kt*CR was discovered with high activity and enantioselectivity. However, other 29 candidates were washed out with little reorganization on the enzymatic properties. Hence a three rounds screening strategy was proposed to recheck the missed reductases. At first, ethyl 4-chloro-3-oxobutanate, a different haloketone to α-chloro-1-acetophenone, was used to retest all 30 reductases. Twelve were returned with activity of more than 0.5 U·mg^{-1}. Five with high enantioselectivity were selected to go through the substrate tolerance assay. Only *Kt*CR, *Dh*CR and *Cg*CR were stable enough and further compared on the enzymatic properties. After rescreening on the thermostability, *Dh*CR and *Cg*CR, with opposite enantioselectivity in the asymmetric reduction of prochiral ketones were identified. At 1 L scale, both could reduce 330 g of **22** into chiral CHBEs, with 92.5% and 93.0% respectively, and >99% *ee*. The S/C ratios were 33 for *Cg*CR and 16.5 for *Dh*CR. Seven chiral halohydrins with pharmaceutical relevance were asymmetrically prepared. All above provide key evidences for the stererocomplementary *Dh*CR and *Cg*CR as potential and robust reductases in organic synthesis.

Experimental

Materials

Prochiral ketones were all from commercial sources (TCI and Aladdin Inc.). Strains used as genome donors were purchased from CGMCC. The pET28a vector was obtained from Novagen (Madison, WI, USA). Competent cells of *E. coli* strains, Dh5α and BL21(DE3), were purchased from TIANGEN (Shanghai, China).

General remarks for gene cloning, expression and purification of proteins

Gene cloning and construction of recombinant plasmids (pET28a-CRs) were reported in our previous work.[18] The *E. coli* BL21(DE3) cells harbouring recombinant pET28a-CRs were cultivated at 37°C in LB medium containing 50 μg·mL^{-1} kanamycin. When the OD_{600} of the culture reached 0.5−0.6, IPTG was added to a final concentration of 0.3 mM, and cultivation was continued at 25°C for a further 15 h. The recombinant *E. coli* BL21(DE3) cells were collected and purified as previously described.[16, 18]

Co-expression of reductase and GDH

The genes coding for *Kt*CR, *Dh*CR and *Cg*CR with independent promoters were separately cut from pET28-*ktcr*, pET28-*dhcr*, pET28-cgcr with *Bgl*II and *Xho*I. The pET28-*bmgdh* vector was digested with *Bam*HI and *Xho*I. Then the fragments of *ktcr*, *dhcr* and *cgcr* with independent promoters were ligated with the above liner pET28-*bmgdh* vector to form pET28-*bmgdh-ktcr*, pET28-bmgdh-dhcr and pET28-*bmgdh-cgcr* plasmids.[25] The resulting plasmids were transformed into *E. coli* BL21 and over-expressed as above mentioned.

Enzyme activity assay

Reductase activity was detected spectrophotometrically at 30°C through monitoring the change of NAD(P)H absorbance at 340 nm. The reaction mixture consisted of 2 μmol substrate (**4** or **22**, unless other stated), 0.1 μmol NADPH or NADH, 50 μmol sodium phosphate buffers (pH 6.5), and an appropriate amount of enzyme in a total volume of 1 mL. One unit of enzyme activity was defined as the amount of enzyme that catalyzed the oxidation of 1 μmol of NADPH per minute under this condition.

Enzyme characterization

The optimum pH of *Kt*CR, *Dh*CR and *Cg*CR was determined in the following buffers (final concentration, 50 mM): sodium citrate (pH 4.0–6.0), sodium phosphate (pH 6.0–8.5), and glycine-NaOH (pH 8.5–10.0) employing above mentioned enzyme activity assay protocol. The optimum temperature was determined under the standard condition at various temperatures (25–80°C). Thermal stability was determined by incubation the purified enzyme (0.1 mg·mL^{-1}) at the desired temperature (30, 40 or 50°C) followed by periodically measuring the residual activity. The kinetic constant analysis of the purified enzyme was performed as previously described.[15]

Conversion and enantioselectivity analysis

The enantioselectivity was determined by examining the reduction of prochiral ketones using NADPH regeneration system consisting of purified reductase and externally added glucose dehydrogenase (GDH). The reactions were carried out in a reaction mixture (0.4 mL) comprising 50 mM sodium phosphate buffer (pH 6.5), 10 mM carbonyl substrates, 0.2 U of the purified reductase, 0.4 U of *Bm*GDH, 20 mM glucose and 0.5 mM $NADP^+$ with shaking for 12 h at 30°C, 900 rpm. Then, each reaction mixture was extracted twice with ethyl acetate. The conversion and ee value were determined by GC analysis equipped with a CP-Chirasil-DEX CB (Varian, USA; 25 m × 0.25 mm × 0.39 mm) column or HPLC analysis using a Chiralcel OD-H column (Daicel Co., Japan; 4.6 × 250 mm) as described in our previous work.[16, 18]

Quantification of intracellular $NADP^+$/NADPH

The intracellular amount of $NADP^+$/NADPH of *E. coli* BL21 was quantified using HPLC (Shimadzu 2010, Shimadzu Scientific Instruments, Japan) equipped with Shim-pack VP-ODS C18 column (Shimadzu Scientific Instruments, Japan; 4.6 mm × 250 mm,). 0.10 g dry cells (or 0.50 g wet cells) of *E. coli* BL21 harbouring pET28a-*bmgdh-dhcr* or pET28a-*bmgdh-cgcr* plasmids was weighted and fully dispersed in 10 mL KPB (pH 7.0, 10 mM). Then the mixture was disrupted with sonication (400 W, work 3 s, intermit 7 s) in ice/water bath and the centrifuged at 12000 rpm for 30 min. After that, the upper aqueous phase was filtered, diluted and went through HPLC, which was performed with 3% acetonitrile aqueous (supplemented with 0.025 mM *N*,*N*,*N*-triethylamine) as mobile phase at 1.0 mL·min^{-1} flow rate at 254 nm and 30°C. The retention times of NAD(H) and NADP(H) were analysed with standards, which were 4.785, 4.555, 7.371 and 8.639 min for $NADP^+$, NAD^+, NADH and NADPH respectively as shown in **Figure S3**.

General protocol for bioconversion

General protocol for the asymmetric reduction of **4** and **22** into optically active α-chloro-1-acetophenol (CAPL) and ethyl 4-chloro-3-hydroxybutanate (CHBE) was carried out by whole cell reaction of *E. coli* harbouring pET28-*bmgdh-ktcr*, pET28-*bmgdh-dhcr* and pET28-*bmgdh-cgcr*. The reaction mixture consisted of 5–10 mL of 1.0 mmol sodium phosphate buffer (pH 6.5), 2.0–20.0 mmol of substrates in 5 mL toluene, 1.5

equiv. glucoses and appropriate dry cells as listed in **Table S6**. The reaction was performed by magnetic agitation at 30°C, 200 rpm and titrated with 2.0 M Na_2CO_3 to maintain the pH at 6.5 until termination. The reaction mixture was centrifuged (8,000 × g for 5 min) to promote the phase separation, and then the aqueous phase was saturated with NaCl and then extracted with ethyl acetate for three times. Then the organic phase was combined with extraction, dried over anhydrous Na_2SO_4 and evaporated under vacuum.

A 1 L reaction mixture of 20 g coexpressed *Bm*GDH & *Dh*CR or 10 g coexpressed *Bm*GDH & *Cg*CR dry cells, and 30.0 g glucose (other 30.0 g was interval added) in 500 mL sodium phosphate buffer (0.1 M, pH 6.5) and an equal volume of toluene in a 3-L mechanical stirred tank reactor were pre-incubated at 30°C for 10 min. Then the reaction was started by adding 330 g of **22**. The pH of reaction mixture was controlled at 6.5 with 2.0 M Na_2CO_3. After stirred at 120 rpm for 24 h, the mixture was extracted with 500 mL ethyl acetate for three times. The organic phase was combined, dried over anhydrous Na_2SO_4 and evaporated under vacuum.

Asymmetric preparations of six *α*-halohydrins were conducted employing the same protocol as COBE (**22**). The reaction mixture was made up of 5–10 mL of 1.0 mmol sodium phosphate buffer (pH 6.5), 2.0–10.0 mmol of substrates in 5 mL toluene, 1.5 equiv. glucoses and appropriate dry cells as listed in **Table 4**. The reaction was performed with magnetic agitation at 30°C, 200 rpm and titrated with 1.0 M Na_2CO_3 to control the pH at 6.5 until completion. Reactions were stopped and extracted as above.

Acknowledgements

This work was financially supported by the National Natural Science Foundation of China (No. 21276082), Ministry of Science and Technology, P. R. China (Nos. 2011CB710800 & 2011AA02A210), China National Special Fund for State Key Laboratory of Bioreactor Engineering (No. 2060204) and Huo Yingdong Education Foundation

Keywords: Genome data mining • Asymmetric reduction • Screening • Stererocomplementary • Halohydrin

Notes and references

[a] State Key Laboratory of Bioreactor Engineering, East China University of Science and Technology, and Shanghai Collaborative Innovation Center for Biomanufacturing Technology Shanghai 200237, China.
[b] The Key Laboratory of Industrial Biotechnology, Ministry of Education, School of Biotechnology, Jiangnan University Wuxi 214122, China.
* Corresponding authors: Dr. H. L. Yu (E-mail: huileiyu@ecust.edu.cn), and Prof. J. H. Xu (E-mail: jianhexu@ecust.edu.cn)

Electronic Supplementary Information (ESI) available: [details of any supplementary information available should be included here]. See DOI: 10.1039/b000000x/

1 a) R. N. Patel, *ACS Catal.* 2011, **1**, 1056–1074; b) J. H. Tao and J. H. Xu, *Curr. Opin. Chem. Biol.*, 2009, **13**, 43–50; c) J. Magano and J. R. Dunetz, *Org. Process Res. Dev.*, 2012, **16**, 1156–1184.
2 a) Z. L. Wei, Z. Y. Li and G. Q. Lin, *Tetrahedron*, 1998, **54**, 13059−13072; b) D. M. Zhu, C. Mukherjee and L. Hua, *Tetrahedron: Asymmetry*, 2005, **16**, 3275−3278; c) N. Itoh, K. Isotani, M. Nakamura, K. Inoue, Y. Isogai and Y. Makino, *Appl. Microbiol. Biotechnol.*, 2012. **93**, 1075–1085.
3 H. Yamamoto, K. Mitsuhashi, N. Kimoto, N. Esaki, Y. Kobayshi, *Biosci. Biotechnol. Biochem.*, 2004, **68**, 638−649.
4 M. Kataoka, L. P. Rohani, K. Yamamoto, H. Kawabata, M. Wada, K. Kita, H. Yanase and S. Shimizu, *Appl. Microbiol. Biotechnol.*, 1999, **41**, 486–490.
5 J. Mangas-Sanchez, E. Busto, V. Gotor-Fernandez, F. Malpartida and V. Gotor, *J. Org. Chem.*, 2011, **76**, 2115−2122.
6 a) A. Schmid, J. S. Dordick, B. Hauer, A. Kiener, M. Wubbolts and B, Witholt, *Nature*, 2001, **409**, 258–268. b) P. T. Anastas and M. M. Kirchhoff, *Acc. Chem. Res.*, 2002, **35**, 686–694; c) J. Clark, R. Sheldon, C. Raston, M. Poliakoff and W. Leitner, *Green Chem.*, 2014, **16**, 18–23.
7 a) H. E. Schoemaker, D. Mink and M. G. Wubbolts, *Science*, 2003, **299**, 1694–1697; b) R. E. Morris and X. H. Bu, *Nat. Chem.*, 2010, **2**, 353–361; c) G. W. Zheng and J. H. Xu, *Curr. Opin. Biotechnol.*, 2011, **22**, 784–792.
8 a) K. Nakamura, R. Yamanaka, T. Matsuda and T. Harada, *Tetrahedron: Asymmetry*, 2003, **14**, 2659−2681; b) H. Gröger, F. Chamouleau, N. Orologas, C. Rollmann, K. Drauz, , W. Hummel, A. Weckbecker and O. May, *Angew. Chem. Int. Ed.*, 2006, **45**, 5677–5681; c) F. Hollmann, I. W. C. E. Arends and D. Holtmann, *Green Chem.*, 2011, **13**, 2285–2313.
9 U. T. Bornscheuer, G. W. Huisman, R. J. Kazlauskas, S. Lutz, J. C. Moore and K. Robins, *Nature*, 2012, **485**, 185–194.
10 C. C. C. R. de Carvalho, *Biotechnol. Adv.*, 2011, **29,** 75–83.
11 a) G. A. Behrens, A. Hummel, S. K. Padhi, S. Schatzle and U. T. Bornscheuer, *Adv. Synth. Catal.*, 2011, **353**, 2191−2215; b) T. Davids, M. Schmidt, D. Bottcher and U. T. Bornscheuer, *Curr. Opin. Chem. Biol.*, 2013, **17**, 215−220.
12 I. Pagani, K. Liolios, J. Jansson, I. M. A. Chen, T. Smirnova, B. Nosrat, V. M. Markowitz and N. C. Kyrpides, *Nucl. Acids Res.*, 2012, **40**, D571−D579.
13 a) S. Z. Zhu, C. Y. Gong, D. W. Song, S. H. Gao and G. J. Zheng, *Appl. Environ. Microbiol.*, 2012, **78**, 7492–7495; b) M. Begley, P. D. Cotter, C. Hill and R. P. Ross, *Appl. Environ. Microbiol.*, 2009, **75**, 5451–5460.
14 S. Luetz, L. Giver and J. Lalonde, *Biotechnol. Bioeng.*, 2008, **101**, 647–653.
15 a) L. J. Wang, C. X. Li, Y. Ni, J. Zhang, X. Liu and J. H. Xu, *Bioresour. Technol.*, 2011, **102**, 7023−7028; b) J. Pan, G. W. Zheng, Q. Ye and J. H. Xu, *Org. Process Res. Dev.*, 2014, **18**, 739–743.
16 H. M. Ma, L. L. Yang, Y. Ni, J. Zhang, C. X. Li, G. W. Zheng, H. Y. Yang and J. H. Xu, *Adv. Synth. Catal.*, 2012, **354**, 1765–1772.

17 N. D. Shen, Y. Ni, H. M. Ma, L. J. Wang, C. X. Li, G. W. Zheng, J. Zhang and J. H. Xu, *Org. Lett.*, 2012, **14**, 1982–1985.
18 G. C. Xu, H. L. Yu, X. Y. Zhang and J. H. Xu, *ACS Catal.*, 2012, **2**, 2566–2571.
19 W. X. Zhang, G. C. Xu, L. Huang, J. Pan, H. L. Yu and J. H. Xu, *Org. Lett.*, 2013, **15**, 4914–4919.
20 J. Li, J. Pan, J. Zhang and J. H. Xu, *J. Mol. Catal. B-Enzymatic*, 2014, **105**, 11–17.
21 H. H. Nguyen-Tran, G. W. Zheng, X. H. Qian and J. H. Xu, *Chem. Commun.*, 2014, **50**, 2861–2864.
22 B. D. Ma, H. L. Yu, J. Pan, J. Y. Liu, X. Ju and J. H. Xu, *Biorecour. Technol.*, 2013, **133**, 354–360.
23 C. S. Zhang, Z. J. Zhang, C. X. Li, H. L. Yu, G. W. Zheng and J. H. Xu, *Appl. Microbiol. Biotechnol.*, 2012, **95**, 91–99.
24 J. Y. Liu, G. W. Zheng, T. Imanaka and J. H. Xu, *Biotechnol. Bioprocess Eng.*, 2014, 19, 442–448.
25 G. C. Xu, H. L. Yu, Z. J. Zhang and J. H. Xu, *Org. Lett.*, 2013, **15**, 5408−5411.
26 Y. P. Xu, Y. H. Guan, H. L. Yu, Y. Ni, B. D. Ma and J. H. Xu, *J. Mol. Catal. B-Enzymatic*, 2014, **104**, 108–114.
27 a) R. D. Mindnich and T. M. Penning, *Hum. Genomic*, 2009, 3, 362–370; b) B. Persson and Y. Kallberg, *Chemico-Biol. Interact.*, 2013, 202, 111–115.
28 a) D. Hyndman, D. R. Bauman, V. V. Heredia and M. Penning, *Chemico-Biol. Interact.*, 2003. **143–144**, 621–631; b) B. Persson, Y. Kallberg, J. E. Bray, E. Bruford, S. L. Dellaporta, A. D. Favia, R. G. Duarte, H. Jörnvall, K. L. Kavanagh, N. Kedishvili, M. Kisiela, E. Maser, R. Mindnich, S. Orchard, T. M. Penning, J. M. Thornton, J. Adamski and U. Oppermann, *Chemico-Biol. Interact.*, 2009, **178**, 94–98.
29 C. Filling, K. D. Berndt, J. Benach, S. Knapp, T. Prozorovski, E. Nordling, R. Ladenstein, H. Jörnvall and U. Oppermann, *J. Biol. Chem.*, 2002, **277**, 25677–25684.
30 L. Di Costanzo, T. M. Penning and D. W. Christianson, *Chemico-Biol. Interact.*, 2009, **178**, 127–133.
31 N. Kizaki, Y. Yasohara, J. Hasegawa, M. Wada, M. Kataoka and S. Shimizu, *Appl. Microbiol. Biotechnol.*, 2001, **55**, 590−595.
32 a) Z. J. Li, L. Cai, Q. Wu and G. Q. Chen, Appl. Microbiol. Biotechnol., 2009, **83**, 929−947; b) H. C. Lee, J. S. Kim, W. Jang and S. Y. Kim, *J. Biotechnol.*, 2010, **149**, 24−32.
33 Y. C. He, Z. C. Tao, X. Zhang, Z. X. Yang and J. H. Xu, *Bioresour. Technol.*, 2014, **161**, 461−464.
34 M. Kataoka, L. P. Rohani, K. Yamamoto, H. Kawabata, M. Wada, K. Kita, H. Yanase and S. Shimizu, *Appl. Microbiol. Biotechnol.*, 1999, **41**, 486−490.
35 Y. Ni, C. X. Li, L. J. Wang, J. Zhang and J. H. Xu, *Org. Biomol. Chem.*, 2011, **9**, 5463−5468.
36 a) M. Kapoor, N. Anand, K. Ahmad, S. Koul, S. S. Chimni, S. C. Taneja and G. N. Qazi, *Tetrahedron: Asymmetry*, 2005, **16**, 717−725; b) T. Fujisawa, K. Ichikawa and M. Shimizu, *Tetrahedron: Asymmetry*, 1993, **4**, 1237–1240; c) J. Nie, H. C. Guo, D. Cahard and J. A. Ma, *Chem. Rev.*, 2011, **111**, 455–529; d) H. Lin, Y. Z. Chen, X. Y. Xu, S. W. Xia and L. X. Wang, *J. Mol. Catal. B-Enzymatic*, 2009, **57**, 1−5; e) P. Krumlinde, K. Bogar and J. E. Bäckvall, *Chem. Eur. J.*, 2010, **16**, 4031−4036; f) X. Rabasseda, L. A. Sorbera and J. Castaner, *Drugs Future*, 1999, **24**, 1057–1067.